5-20-2020

Computational Study of the Time Relaxation Model With High Order Deconvolution Operator

Jeffrey Belding
University of Nevada, Las Vegas

Monika Neda
University of Nevada, Las Vegas, monika.neda@unlv.edu

Fran Pahlevani
Penn State University

Repository Citation

Belding, J., Neda, M., Pahlevani, F. (2020). Computational Study of the Time Relaxation Model With High Order Deconvolution Operator. *Results in Applied Mathematics* 1-16.
http://dx.doi.org/10.1016/j.rinam.2020.100111

ARTICLE IN PRESS

Results in Applied Mathematics xxx (xxxx) xxx

Contents lists available at ScienceDirect

Results in Applied Mathematics

journal homepage: www.elsevier.com/locate/results-in-applied-mathematics

Computational study of the Time Relaxation Model with high order deconvolution operator

Jeffrey Belding [a], Monika Neda [a], Fran Pahlevani [b,*]

[a] Department of Mathematics, University of Nevada, Las Vegas, NV, 89154, United States of America
[b] Department of Mathematics, Penn State University - Abington College, PA, 19001, United States of America

ARTICLE INFO

Article history:
Received 3 December 2019
Received in revised form 16 April 2020
Accepted 23 April 2020
Available online xxxx

ABSTRACT

This paper presents a computational investigation for a time relaxation regularization of Navier–Stokes equations known as Time Relaxation Model, TRM, and its corresponding sensitivity equations. The model generates a regularization based on both filtering and deconvolution. We discretize the equations of TRM and the corresponding sensitivity equations using finite element in space and Crank–Nicolson in time. The step problem and the shear layer roll-up benchmark is used to computationally test the performance of TRM across different orders of deconvolution operator as well as the sensitivity of the shear layer computations of the model with respect to the variation of time relaxation parameter in those cases.

1. Introduction

The study of fluid flow is important to a broad range of practical problems related to various fields. It is known that the flow consists of different size structures on the order of $O(Re^{-3/4})$, where Reynold's number $Re \sim 1/\nu$ with ν denoting the kinematic viscosity. A direct numerical simulation of a 3d turbulent flow requires $O(Re^{9/4})$ mesh points in space per time step. For high Reynolds numbers, this becomes computationally challenging and typically not feasible. Large eddy simulation is a promising alternative that aims to truncate the small scales and model their effect upon the solution. Among different fluid models produced by this idea, high order models are of interest, since they deliver a more accurate simulation at low model resolution. Unfortunately most of these different types of models have the chance of altering the largest structures of the flow that contain most of the flow's energy and are responsible for most of the mixing and flow's momentum transport [1].

In the present paper, computations of fluid flow based on TRM and their sensitivity are performed using the shear layer roll-up test problem and the step problem. The idea of TRM was first introduced by Stolz, Adams and Kleiser [2,3]. The truncation scale analysis of this model is shown in [1]. Further numerical studies and computational accuracy of TRM can be found in [1,4–6]. The analysis of TRM parameter sensitivity was performed in [7,8].

The governing equations for TRM are formulated as follows:

$$\begin{aligned} \mathbf{u}_t + \mathbf{u}\cdot\nabla\mathbf{u} - \nu\Delta\mathbf{u} + \nabla p + \chi(\mathbf{u} - G_N\bar{\mathbf{u}}) &= \mathbf{f}, \quad \forall (x,t) \in \Omega \times [0,T], \\ \nabla\cdot\mathbf{u} &= 0, \quad \forall (x,t) \in \Omega \times [0,T]. \end{aligned} \tag{1.1}$$

* Corresponding author.
E-mail addresses: jeffrey.belding@unlv.edu (J. Belding), monika.neda@unlv.edu (M. Neda), fxp10@psu.edu (F. Pahlevani).

https://doi.org/10.1016/j.rinam.2020.100111

Please cite this article as: J. Belding, M. Neda and F. Pahlevani, Computational study of the Time Relaxation Model with high order deconvolution operator. Results in Applied Mathematics (2020) 100111, https://doi.org/10.1016/j.rinam.2020.100111.

where Ω is our domain of interest in $\mathbb{R}^d$, $(d = 2, 3)$, χ is a scalar constant known as the relaxation parameter, and $\bar{\mathbf{u}}$ denotes a spatially averaged function of $\mathbf{u}$ defined as: $\bar{\mathbf{u}} := G(\mathbf{u})$, which is the solution of the partial differential equation:

$$\begin{aligned} -\delta^2 \Delta \bar{\mathbf{u}} + \bar{\mathbf{u}} &= \mathbf{u}, \text{ in } \Omega, \\ \bar{\mathbf{u}} &= \mathbf{0}, \text{ on } \partial\Omega. \end{aligned} \tag{1.2}$$

In the above filtering equation, δ is a constant corresponding to the filter width. Thus for large δ values, $\bar{\mathbf{u}}$ is smooth and for small δ values, $\bar{\mathbf{u}}$ is close to $\mathbf{u}$.

The operator G_N in (1.1) represents the Nth van Cittert approximate deconvolution operator. This operator was first studied by van Cittert in 1931. For each $N = 0, 1, \ldots$ it computes an approximate solution $\mathbf{u}_N$ to the above filtering equation by a fixed point iteration of N steps [9]. The process is as follows: first rewrite the deconvolution equation $\bar{\mathbf{u}} = G(\mathbf{u})$ as the following fixed point problem: Given $\bar{\mathbf{u}}$, solve $\mathbf{u} = \mathbf{u} + (\bar{\mathbf{u}} - G\mathbf{u})$.

We can now solve for the deconvolution approximation using the following algorithm:

$$\begin{aligned} &\mathbf{u}_0 = \bar{\mathbf{u}}, \\ &\mathbf{u}_{n+1} = \mathbf{u}_n + (\bar{\mathbf{u}} - G\mathbf{u}_n), \quad n = 1, 2, 3, \ldots, N-1. \end{aligned} \tag{1.3}$$

This algorithm is precisely the first order Richardson iteration for the operator equation $\bar{\mathbf{u}} = G(\mathbf{u})$, where $G : (L^2(\Omega))^d \longrightarrow (L^2(\Omega))^d$ is the operator given above, which is possibly non-invertible. The de-convolution problem is ill-posed, so we cannot expect such an algorithm to converge as $N \to \infty$. With these preliminaries, we can now define the operator G_N which appears in (1.1):

Definition 1.1. The Nth van Cittert approximate deconvolution operator $G_N : (L^2(\Omega))^d \longrightarrow (L^2(\Omega))^d$ is the map $G_N : \bar{\mathbf{u}} \longrightarrow \mathbf{u}_N$, or $G_N(\bar{\mathbf{u}}) = \mathbf{u}_N$.

It is an easy exercise to find the following explicit formula for the deconvolution operator G_N:

$$G_N \bar{\mathbf{u}} := \sum_{n=0}^{N} (I - G)^n \bar{\mathbf{u}}, \quad N = 0, 1, 2, \ldots . \tag{1.4}$$

For convenience, we list the first few values of the G_N operator here:

$$\begin{aligned} &G_0 \bar{\mathbf{u}} = \bar{\mathbf{u}}, \\ &G_1 \bar{\mathbf{u}} = 2\bar{\mathbf{u}} - \bar{\bar{\mathbf{u}}}, \\ &G_2 \bar{\mathbf{u}} = 3\bar{\mathbf{u}} - 3\bar{\bar{\mathbf{u}}} + \bar{\bar{\bar{\mathbf{u}}}}. \end{aligned}$$

The time relaxation parameter is considered to be a positive quantity, i.e. $\chi > 0$, and has units of $1/time$. The term $\chi(\mathbf{u} - G_N \bar{\mathbf{u}})$ aims to drive the unresolved scales to zero exponentially [10]. In working with TRM, the parameter χ must be specified and scaled appropriately in relation to other parameters in the problem [1].

1.1. The effective averaging length scale

In this section, based on Olson's work in [11], we identify the effective averaging length scale in the TRM model as $\delta_N = \delta_0 \sqrt{N+1}$, where δ_0 is a fixed length scale suited for the $N = 0$ version of our model. Following the work from Olson, we consider the effects of the deconvolution filter for the time relaxation term $\chi(u - G_N \bar{u})$ on regular 2π-periodic functions with a spatial average of 0 in Fourier Space. Hence, we can write the following forms for u and $\bar{u}$:

$$u(x, t) = \sum_{k \in \mathbf{Z}^d \setminus 0} u_k(t) e^{ik \cdot x} \quad \text{and} \quad \bar{u}(x, t) = \sum_{k \in \mathbf{Z}^d \setminus 0} \bar{u}_k(t) e^{ik \cdot x}.$$

It follows from the differential filter (1.2) and deconvolution algorithm (1.3) that

$$G_N \bar{u}_k = G_{N,k} (1 + \delta^2 |k|^2)^{-1} u_k,$$

where

$$G_{N,k} = \sum_{n=0}^{N} \left(1 - \frac{1}{1 + \delta^2 |k|^2}\right)^n = \sum_{n=0}^{N} \left(\frac{\delta^2 |k|^2}{1 + \delta^2 |k|^2}\right)^n.$$

Noting that the above is a geometric series, we sum up the above series to obtain:

$$\frac{G_{N,k}}{1 + \delta^2 |k|^2} = 1 - \left(\frac{\delta^2 |k|^2}{1 + \delta^2 |k|^2}\right)^{N+1}.$$

Please cite this article as: J. Belding, M. Neda and F. Pahlevani, Computational study of the Time Relaxation Model with high order deconvolution operator. Results in Applied Mathematics (2020) 100111, https://doi.org/10.1016/j.rinam.2020.100111.

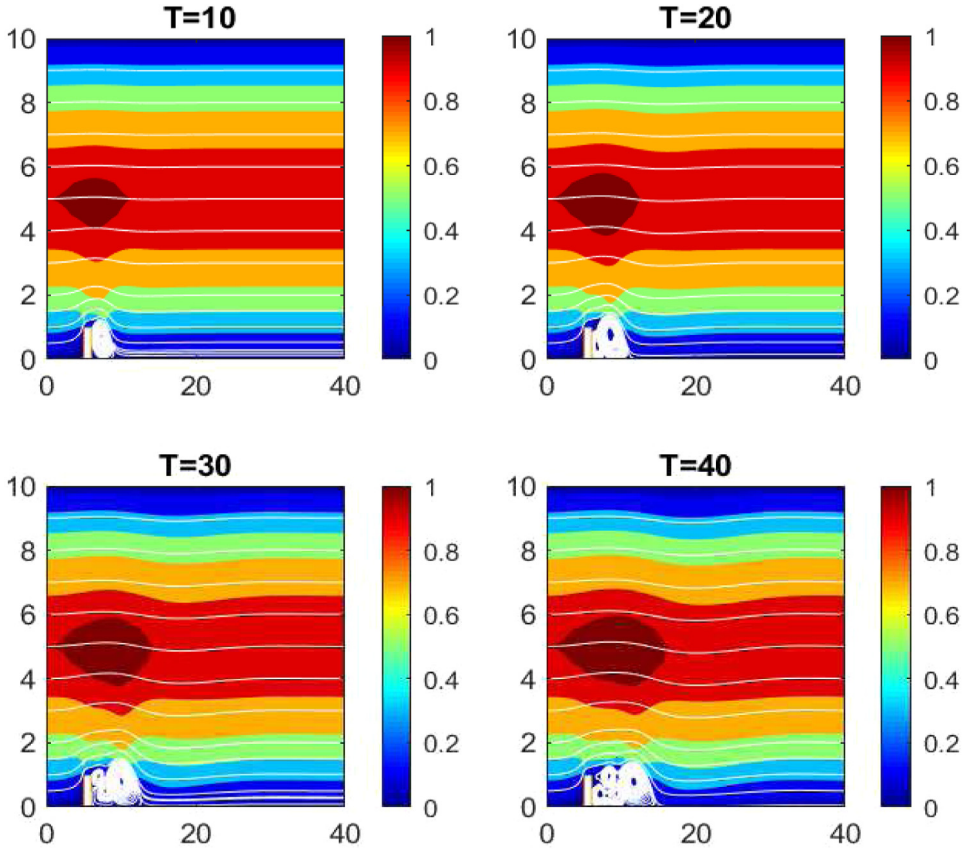

Fig. 1. NSE at $\nu = 1/600$ and on fine mesh level 2.

For the LHS of above, we note the following limits

$$\frac{G_{N,k}}{1+\delta^2|k|^2} \to 1 \text{ as } N \to \infty \text{ for fixed } \delta, \text{ or as } \delta \to 0 \text{ for fixed N.}$$

Also,

$$\frac{G_{N,k}}{1+\delta^2|k|^2} \to 0 \text{ as } \delta \to \infty \text{ for fixed } N.$$

These limits suggest that there is a relationship between δ and N which can be used to identify an effective averaging length scale that leaves the small scale attenuation of the smoothing filter unchanged as we increase the order of convolution N. Now we do asymptotic analysis on the term $G_{N,k}/(1+\delta^2|k|^2)$ as $k \to \infty$ to determine this relationship for the averaging length scale. We have that

$$\frac{G_{N,k}}{1+\delta^2|k|^2} = 1 - \left(\frac{\delta^2|k|^2}{1+\delta^2|k|^2}\right)^{N+1} \sim \frac{N+1}{\delta^2|k|^2} \quad \text{for large } k.$$

From this behavior, it is clear that if we scale our δ for higher N values as $\delta_N = \delta_0\sqrt{N+1}$ for some chosen constant δ_0 for $N = 0$, we obtain an asymptotic decay for the above expression that is independent of N as $k \to \infty$. This choice of delta for higher N will be apparent in the benchmark problem we pursue in a later section of this paper.

2. Preliminaries and notations

This section presents the finite element notation, preliminary results, and the finite element schemes in order to numerically solve (1.1) and (1.2). The $L^2(\Omega)$ norm and inner product will be denoted by $\|\cdot\|$ and $(\cdot,\cdot)$. Likewise, the $L^p(\Omega)$ norms and the Sobolev $W_p^k(\Omega)$ norms are denoted by $\|\cdot\|_{L^p}$ and $\|\cdot\|_{W_p^k}$, respectively. For the semi-norm in $W_p^k(\Omega)$ we use $|\cdot|_{W_p^k}$. H^k is used to represent the Sobolev space W_2^k, and $\|\cdot\|_k$ denotes the norm in H^k. For functions $\mathbf{v}(\mathbf{x}, t)$ defined

Please cite this article as: J. Belding, M. Neda and F. Pahlevani, Computational study of the Time Relaxation Model with high order deconvolution operator. Results in Applied Mathematics (2020) 100111, https://doi.org/10.1016/j.rinam.2020.100111.

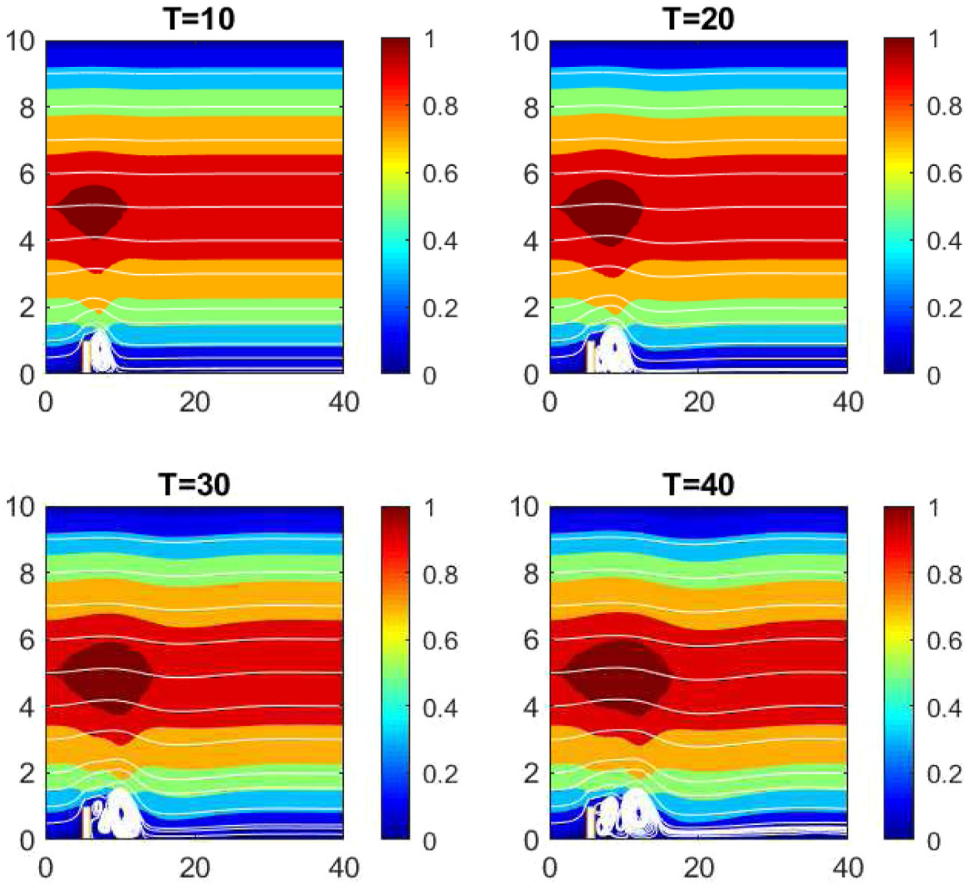

Fig. 2. NSE at $\nu = 1/600$ and on coarse mesh level 1.

on the entire time interval $(0, T)$, we define

$$\|\mathbf{v}\|_{\infty,k} := \sup_{0<t<T} \|\mathbf{v}(t,\cdot)\|_k, \qquad \text{and} \qquad \|\mathbf{v}\|_{m,k} := \left(\int_0^T \|\mathbf{v}(t,\cdot)\|_k^m \, dt\right)^{1/m}.$$

The velocity and pressure finite element spaces (X^h, Q^h) are defined respectively,

$$X^h \subset X = H_0^1(\Omega) := \{\mathbf{v} \in H^1(\Omega)^d : \ \mathbf{v}|_{\partial\Omega} = 0\},$$
$$Q^h \subset Q = L_0^2(\Omega) := \{q \in L^2(\Omega) | \int_\Omega q = 0\},$$

and the space of discretely divergence free velocity is

$$V^h = \{\mathbf{v} \in X^h : (q, \nabla \cdot \mathbf{v}) = 0, \forall q \in Q^h\}.$$

We assume that the spaces X^h, Q^h satisfy the discrete inf–sup condition. Also, bilinear $a(\cdot,\cdot) : X \times X \to \mathbb{R}$ and trilinear $b^*(\cdot,\cdot,\cdot) : X \times X \times X \to \mathbb{R}$ forms are defined as,

$$a(\mathbf{u}, \mathbf{v}) := (\nabla \mathbf{u}, \nabla \mathbf{v}),$$
$$b^*(\mathbf{u}, \mathbf{v}, \mathbf{w}) := \frac{1}{2}(\mathbf{u} \cdot \nabla \mathbf{v}, \mathbf{w}) - \frac{1}{2}(\mathbf{u} \cdot \nabla \mathbf{w}, \mathbf{v}).$$

We will also need to define discretized versions of our filtering equation and the deconvolution operator. Following the lead of Manica and Kaya-Merdan [12], the discretized differential filtering equation is as follows: For $\phi \in L^2(\Omega)$ and a given filtering radius $\delta > 0$, we define the operator $G^h : L^2(\Omega) \longrightarrow L^2(\Omega)$ by the equation $\overline{\phi}^h := G^h(\phi)$, where $\overline{\phi}^h$ is the unique solution of the following variational formulation:

$$\delta^2(\nabla \overline{\phi}^h, \nabla v_h) + (\overline{\phi}^h, v_h) = (\phi, v_h), \quad \forall v_h \in X_h. \tag{2.1}$$

Please cite this article as: J. Belding, M. Neda and F. Pahlevani, Computational study of the Time Relaxation Model with high order deconvolution operator. Results in Applied Mathematics (2020) 100111, https://doi.org/10.1016/j.rinam.2020.100111.

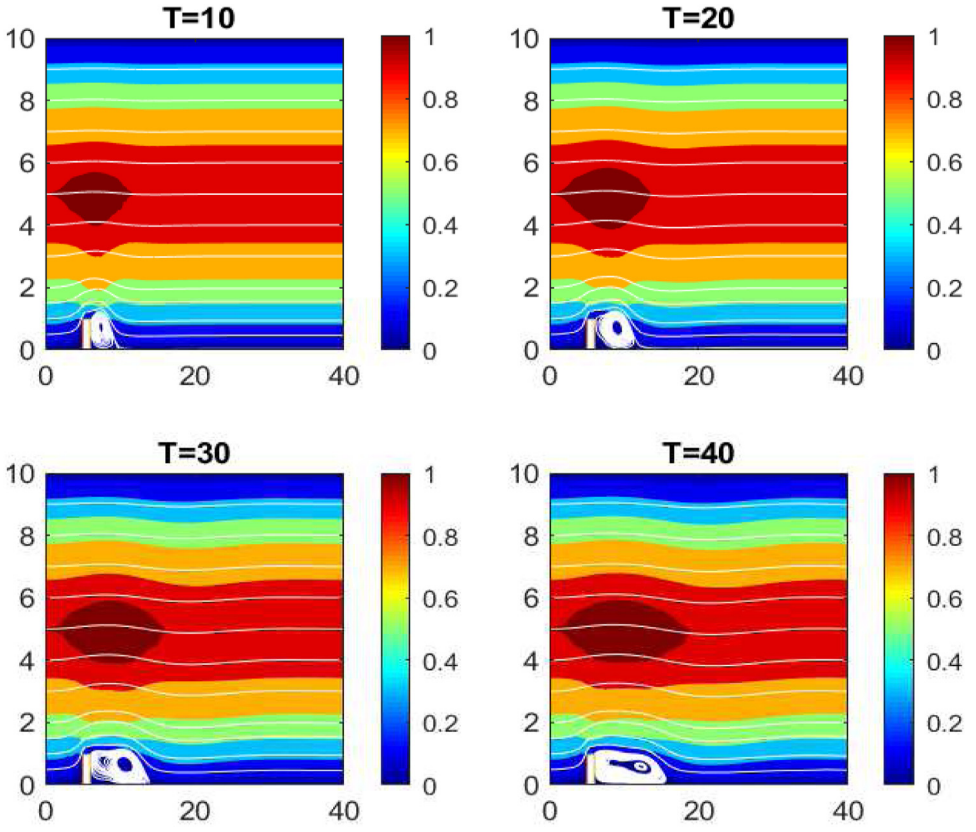

Fig. 3. TRM with N=0, δ_0, at $\nu = 1/600$ and on coarse mesh level 1.

Another possibility for defining the differential filter is to instead use a Stokes problem. This is of course a more expensive filtering operation. But, such an approach allows us to preserve the incompressibility approximately for the filtered velocity in the non-periodic cases [13–15]. Thus, for the case of internal flows under the no-slip boundary conditions, we will choose the discrete Stokes differential filter to weakly preserve the incompressibility of the filtered velocity. In this case, for any $\phi \in X'$ and $\delta > 0$, we define $G^h : X' \longrightarrow X_h$ by $\overline{\phi}^h = G^h(\phi)$, where $(\overline{\phi}^h, \rho) \in X_h \times P_h$ is the unique solution of the following variational formulation:

$$\begin{aligned} \delta^2(\nabla\overline{\phi}^h, \nabla v_h) + (\overline{\phi}^h, v_h) - (\rho, \nabla \cdot v_h) &= (\phi, v_h), \quad \forall v_h \in X_h, \\ (\nabla \cdot \overline{\phi}^h, q) &= 0, \quad \forall q \in P_h. \end{aligned}$$

Note that the Stokes filter gives us a weakly divergence free filtered velocity, and therefore the discrete Stokes filtered velocity is also weakly divergence free in the discrete sense. Now that we have defined a discretized differential filter, the same procedure used in the continuous case can be used here to define a discrete Nth van Cittert deconvolution operator.

Definition 2.1. The discrete Nth order van Citter deconvolution operator G_N^h is defined by the following formula:

$$G_N^h \phi := \sum_{n=0}^{N} (I - G^h)^n \phi, \quad N = 0, 1, 2, \ldots. \tag{2.2}$$

It can be shown that both G_N and G_N^h are $O(\delta^{2N+2})$ inverse approximates to the filter operators G and G^h respectively . Both proofs are based on the same type of algebraic manipulations, and can be found in [16,17].

3. Variational formulation and the computational algorithm

The variational formulation of TRM based on the set of Eqs. (1.1)–(1.2) using suitable choice of test functions from X and Q are respectively given as: Find $(\mathbf{u}, p) \in (X, Q)$ such that:

$$(\mathbf{u}_t, \mathbf{v}) + \nu a(\mathbf{u}, \mathbf{v}) + b^*(\mathbf{u}, \mathbf{u}, \mathbf{v}) - (p, \nabla \cdot \mathbf{v}) + \chi(\mathbf{u} - G_N\bar{\mathbf{u}}, \mathbf{v}) = (\mathbf{f}, \mathbf{v}), \quad \forall \mathbf{v} \in X, \tag{3.1}$$

Please cite this article as: J. Belding, M. Neda and F. Pahlevani, Computational study of the Time Relaxation Model with high order deconvolution operator. Results in Applied Mathematics (2020) 100111, https://doi.org/10.1016/j.rinam.2020.100111.

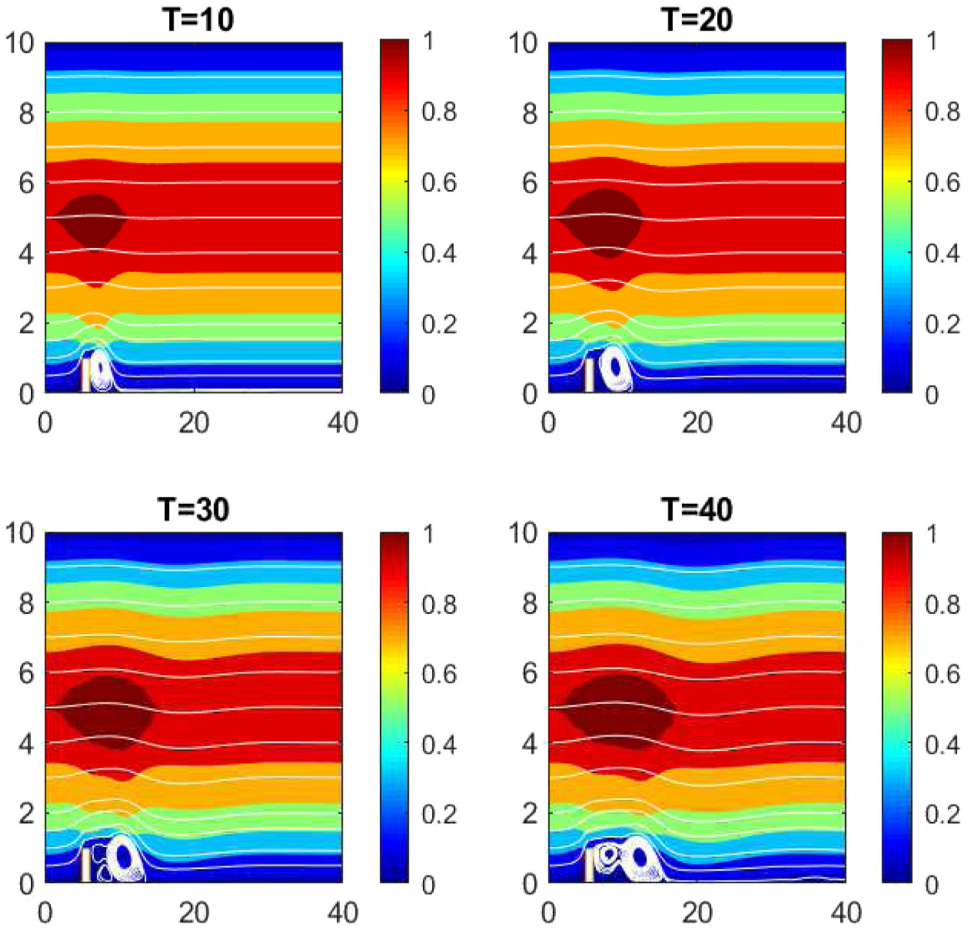

Fig. 4. TRM with N=1, unscaled δ_0, at $\nu = 1/600$ and on coarse mesh level 1.

$$(\nabla \cdot \mathbf{u}, q) = 0, \quad \forall q \in Q, \tag{3.2}$$

$$\delta^2(\nabla \bar{\mathbf{u}}, \nabla \mathbf{v}) + (\bar{\mathbf{u}}, \mathbf{v}) = (\mathbf{u}, \mathbf{v}), \quad \forall \mathbf{v} \in X. \tag{3.3}$$

The method of Crank–Nicolson is used for time discretization. Our notations in the time discretization equations of TRM read as following: $v(t^{n+1/2}) = v((t^{n+1} + t^n)/2)$ for the continuous variable and $v^{n+1/2} = (v^{n+1} + v^n)/2$ for both, continuous and discrete variables. Thus, the fully discretized finite element variational formulation of TRM is written as follows.

Given (X^h, Q^h), the time interval $[0, T]$, the time step chosen as $\triangle t < T = M \triangle t$, find the approximated TRM solution $(\mathbf{u}_h^{n+1}, p_h^{n+1}) \in (X^h, Q^h)$, for $n = 0, 1, 2....M - 1$ satisfying:

$$\frac{1}{\triangle t}(\mathbf{u}_h^{n+1} - \mathbf{u}_h^n, \mathbf{v}_h) + \nu a(\mathbf{u}_h^{n+1/2}, \mathbf{v}_h) + b^*(\mathbf{u}_h^{n+1/2}, \mathbf{u}_h^{n+1/2}, \mathbf{v}_h) - (p_h^{n+1}, \nabla \cdot \mathbf{v}_h)$$
$$+ \chi(\mathbf{u}_h^{n+1/2} - G_N^h \overline{\mathbf{u}_h^{n+1/2}}^h, \mathbf{v}_h) = (\mathbf{f}^{n+1/2}, \mathbf{v}_h), \quad \forall \mathbf{v}_h \in X^h, \tag{3.4}$$

$$(\nabla \cdot \mathbf{u}_h^{n+1}, q_h) = 0, \quad \forall q_h \in Q^h, \tag{3.5}$$

$$\delta^2(\nabla \bar{\mathbf{u}}_h^{n+1}, \nabla \mathbf{v}_h) + (\bar{\mathbf{u}}_h^{n+1}, \mathbf{v}_h) = (\mathbf{u}_h^{n+1}, \mathbf{v}_h), \quad \forall \mathbf{v}_h \in X^h. \tag{3.6}$$

In the space V^h, Eqs. (3.4)–(3.6) are equivalently rewritten as follows.
Find $\mathbf{u}_h^{n+1} \in V^h$, for $n = 0, 1, 2....M - 1$ satisfying:

$$\frac{1}{\triangle t}(\mathbf{u}_h^{n+1} - \mathbf{u}_h^n, \mathbf{v}_h) + \nu a(\mathbf{u}_h^{n+1/2}, \mathbf{v}_h) + b^*(\mathbf{u}_h^{n+1/2}, \mathbf{u}_h^{n+1/2}, \mathbf{v}_h)$$
$$+ \chi(\mathbf{u}_h^{n+1/2} - G_N^h \overline{\mathbf{u}_h^{n+1/2}}^h, \mathbf{v}_h) = (\mathbf{f}^{n+1/2}, \mathbf{v}_h), \quad \forall \mathbf{v}_h \in V^h, \tag{3.7}$$

$$\delta^2(\nabla \bar{\mathbf{u}}_h^{n+1}, \nabla \mathbf{v}_h) + (\bar{\mathbf{u}}_h^{n+1}, \mathbf{v}_h) = (\mathbf{u}_h^{n+1}, \mathbf{v}_h), \quad \forall \mathbf{v}_h \in V^h. \tag{3.8}$$

Please cite this article as: J. Belding, M. Neda and F. Pahlevani, Computational study of the Time Relaxation Model with high order deconvolution operator. Results in Applied Mathematics (2020) 100111, https://doi.org/10.1016/j.rinam.2020.100111.

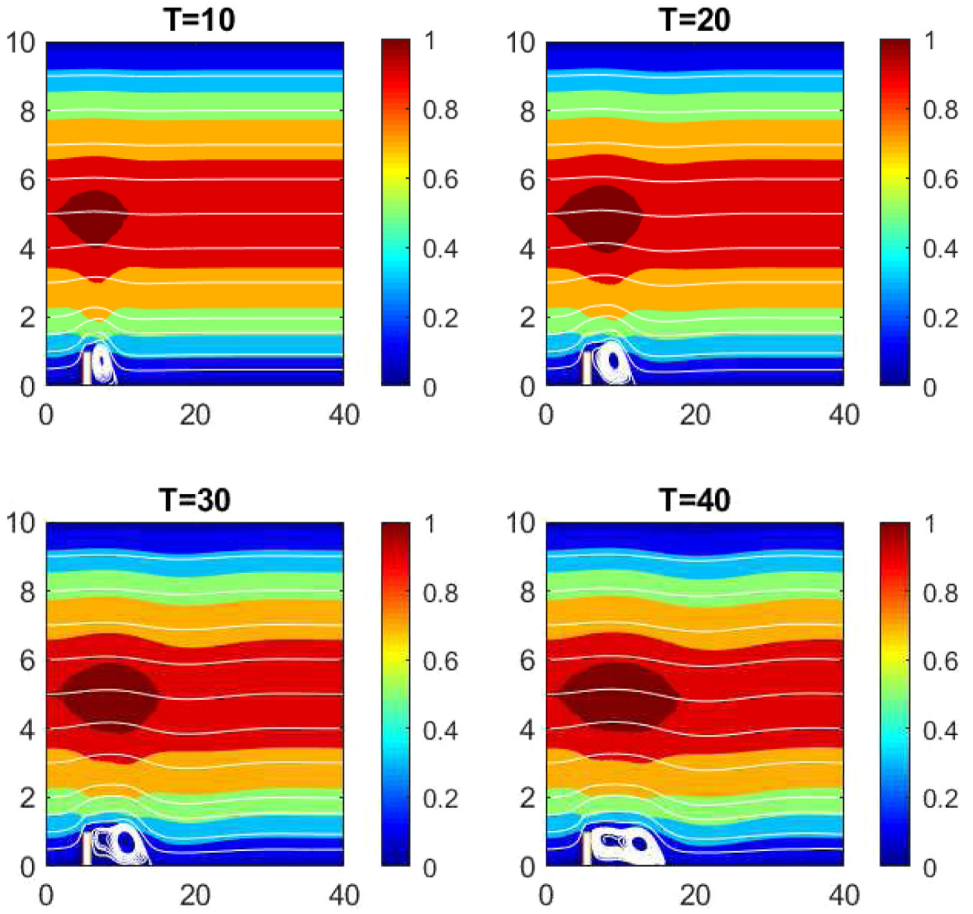

Fig. 5. TRM with N=1, scaled δ_1, at $\nu = 1/600$ and on coarse mesh level 1.

The existence, stability, and convergence analysis of the finite element solution of the above schemes are investigated in [10]. In our computations, the non-linear term $b^*(\mathbf{u}_h^{n+1/2}, \mathbf{u}_h^{n+1/2}, \mathbf{v}_h)$ in Eq. (3.7) is approximated by the method of fixed point iteration. We implemented the Stokes filter for all our computations.

4. Computational results

This section contains computational results for two benchmark problems: step problem and shear layer roll-up problem. We tested our model TRM with different order of deconvolutions, such as $N = 0$, $N = 1$ and $N = 2$. In the cases for higher order of deconvolution, we tested the unscaled and scaled filter length based on its derivation in Section 1.1.

4.1. Computations for step problem

We present herein a benchmark flow with recirculation, the so called flow across a step. The most distinctive characteristic of this fluid flow is the development of a recirculating vortex behind the step around Reynolds number $Re = 600$, see [18]. We will study this flow in the transition via shedding of eddies behind the step using our model, i.e. (3.1)–(3.3) with $N = 0$, $N = 1$ and $N = 2$. The domain of this problem is a 40×10 channel with a 1×1 step size situated five units into the channel at the bottom border. Our results are for a parabolic inflow profile, which is given by $u = (u_1, u_2)^T$, with $u_1 = y(10 - y)/25$, $u_2 = 0$. This profile is also imposed at the outflow while no-slip boundary condition is prescribed on the top, bottom boundary and around the step borders. The computations were performed on two different meshes: coarse mesh level 1 (with 8348 dof) and fine mesh level 2 (with 38,451 dof). The goal is to compare the performance of the various cases in underresolved simulations by comparison against the truth solution. We used the $P3/P2$ finite element spaces, i.e. third order polynomial approximations for velocity and second order polynomial approximations for pressure. We set our kinematic viscosity $\nu = 1/600$. The filter width is chosen to be of order of the mesh size elements behind the step. The background color represents the norm of the velocity vectors. Fig. 1 shows the successful replication of the shedding of eddies that represents our true solution for this problem.

Please cite this article as: J. Belding, M. Neda and F. Pahlevani, Computational study of the Time Relaxation Model with high order deconvolution operator. Results in Applied Mathematics (2020) 100111, https://doi.org/10.1016/j.rinam.2020.100111.

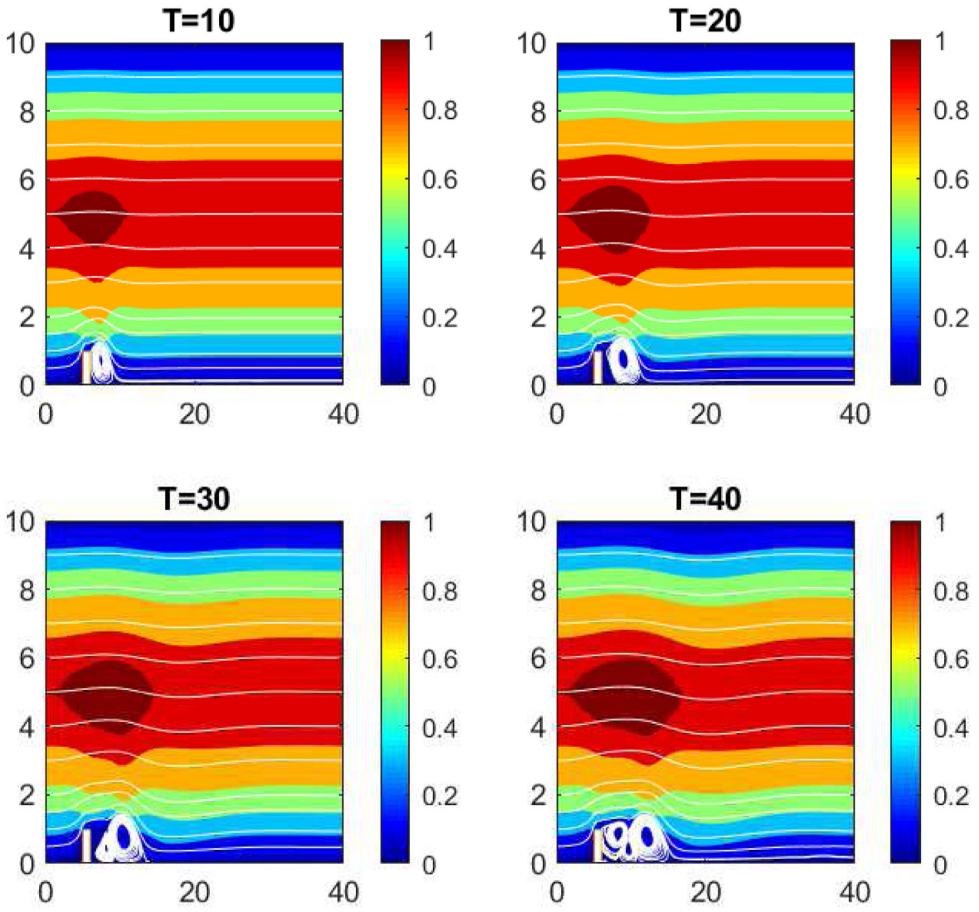

Fig. 6. TRM with N=2, unscaled δ_0, at $\nu = 1/600$ and on coarse mesh level 1.

Fig. 2 shows the Navier–Stokes solution on the coarse mesh level 1 where oscillations are present at later times. On the same mesh level, Figs. 3–5, 6 and 7 give qualitative results with eddies behind the step that are recognizable for our model. These figures were obtained for $\chi = 0.1$ and $\delta_0 = 0.25$. For values of scaled filter width for order of deconvolution $N = 1$ we had $\delta_1 = \delta_0\sqrt{2}$ and for $N = 2$ we had $\delta_2 = \delta_0\sqrt{3}$. Clearly, increasing order of deconvolution helps in reducing the stabilizing effects of the time relaxation term and starts to give the appearance of more than one eddy behind the step. In the simulations for $N = 0$ we do not have the phenomenon of shedding of the eddies, while for higher order of deconvolution $N = 1$ and $N = 2$ we do observe eddy shedding behind the step.

We could not obtain the Navier–Stokes solution at $\nu = 1/10{,}000$ neither on mesh level 1 nor mesh level 2 due to the mesh being too coarse for this Reynold's number. This is theoretically explained by the Kolmogorov theory that says that we need to have much finer mesh when we increase the Reynolds number. The nonlinear Oseen type of iteration failed to converge at the 42nd time iteration on the fine mesh level 2 and at the 171st time iteration on the coarse mesh level 1. The convergence tolerance for the Oseen type of the problem was set to 10^{-5}. Then, we investigated our model on the coarse mesh level 1. When we ran our model TRM with $\chi = 0.7$ and $\delta = 0.25$ for scaled $N = 1$ and scaled $N = 2$, we obtained a meaningful flow, as well as for $N = 0$. This is presented in Fig. 8 for the order of deconvolution $N = 1$ and we omitted the cases for $N = 0$ and $N = 2$ since they gave an identical qualitative output. We captured the rotational structure behind the step but we did not get shedding of the eddies. The TRM for $N = 1$ and $N = 2$ with unscaled filter width failed to converge at the 475th time iteration and at the 381st time iteration, respectively.

4.2. Computations for shear layer problem and its sensitivity

This section contains computations for approximated velocity using TRM with deconvolution orders of $N = 0$, 1, and 2 for the so called shear layer roll-up test problem. The sensitivity computations with respect to the variations of time relaxation parameter χ for all the tested deconvolution orders are performed as well.

Please cite this article as: J. Belding, M. Neda and F. Pahlevani, Computational study of the Time Relaxation Model with high order deconvolution operator. Results in Applied Mathematics (2020) 100111, https://doi.org/10.1016/j.rinam.2020.100111.

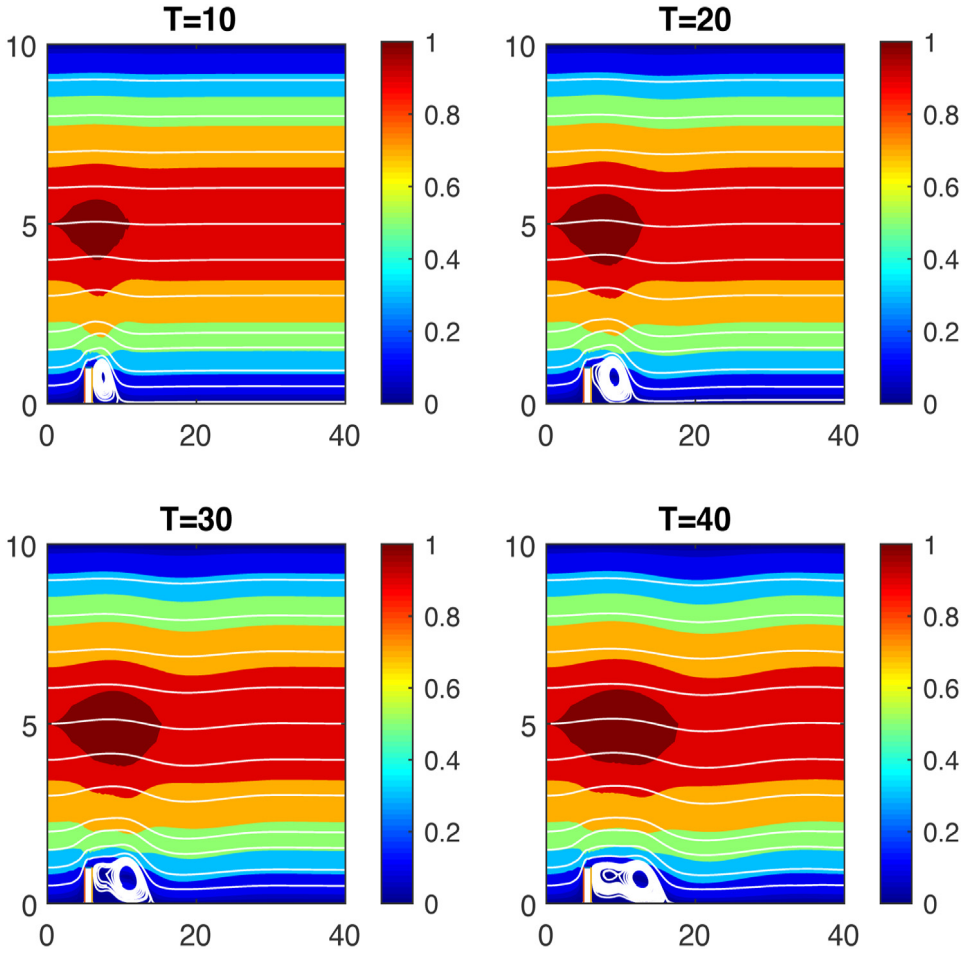

Fig. 7. TRM with N=2, scaled δ_2, at $\nu = 1/600$ and on coarse mesh level 1.

4.2.1. Shear layer roll-up benchmark

This is a benchmark problem involving a doubly periodic pair of shear layers studied in [19–21]. The initial flow field consists of a horizontal shear layer of finite thickness, perturbed by a small amplitude vertical velocity. Each of the shear layers forming the boundaries of the initial jet will eventually evolve into a periodic array of large vortices. Meanwhile, the shear layers between the rolls are thinned out by the large straining field, which then causes these layers to wrap around the large rolls. An exact solution is not known for this problem, thus a reference solution is generated for the problem using a very fine mesh and will be used to test for the accuracy of our simulations. The domain is $\Omega = [0, 1]^2$, and initial conditions are given by

$$u = \begin{cases} \tanh(\rho(y - 0.25)) & \text{if } y \leq 0.5, \\ \tanh(\rho(0.75 - y)) & \text{if } y > 0.5, \end{cases}$$
$$v = \delta \sin(2\pi x).$$

Doubly-periodic boundary conditions are applied on our domain Ω. The time step $\triangle t = 0.004$, Reynolds number $Re = 10{,}000$ (i.e. $\nu = 1/10{,}000$), Taylor–Hood finite elements, and uniform triangular mesh, were used in all cases. The relaxation parameters used are $\chi = 0.1$ and $\chi = 1$ and the shear layer width parameter $\rho = 80$, while the filter radius is given by the scaled values $\delta_N = \delta_0\sqrt{N+1}$ with $\delta_0 = \frac{5}{m}$, where m denotes the number of subintervals on each side of the square domain Ω. Thus, the filter width for TRM with order of deconvolution $N = 0$ is denoted by δ_0, for TRM with $N = 1$ the scaled filter width is given by $\delta_1 = \delta_0\sqrt{2}$, and for TRM with $N = 2$ we have the scaled filter width $\delta_2 = \delta_0\sqrt{3}$. The initial condition vector field is plotted in Fig. 9.

We present the true unfiltered vorticity solution (i.e. Navier–Stokes solution) obtained on a fine mesh with $m = 250$ in Fig. 10. Then, the simulations from Figs. 11 and 13 are on a coarse mesh with $m = 100$. These vorticity plots show the advantage of applying the time relaxation modeling in comparison with no filtering and deconvolution, i.e. a

Please cite this article as: J. Belding, M. Neda and F. Pahlevani, Computational study of the Time Relaxation Model with high order deconvolution operator. Results in Applied Mathematics (2020) 100111, https://doi.org/10.1016/j.rinam.2020.100111.

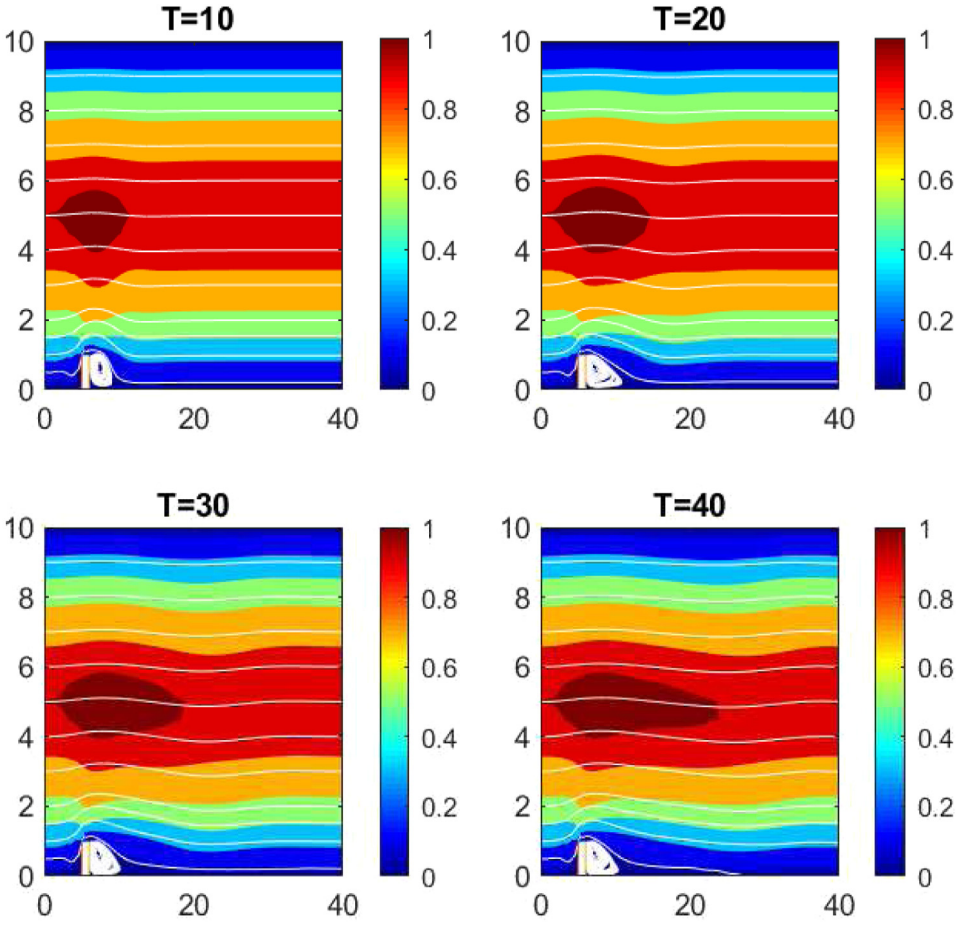

Fig. 8. TRM with N=1, scaled δ_1, at $\nu = 1/10{,}000$ and on coarse mesh level 1.

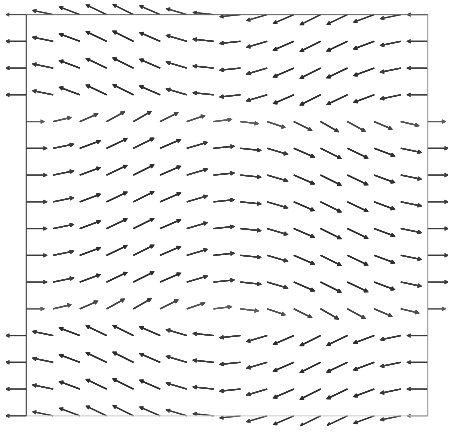

Fig. 9. Initial Velocity field for the Shear Layer problem, with $\rho = 80$, $\delta = 0.5$.

Navier–Stokes solution that has more spurious vortices on the coarse mesh, especially as the vorticity develops in time. In Figs. 12 and 14 we can see the advantage of using scaled values for the filter width over the constant value δ_0 as we increase the order of deconvolution N. The produced vorticity plots for scaled values of the filter width had less noise and increased accuracy compared to the true solution.

Please cite this article as: J. Belding, M. Neda and F. Pahlevani, Computational study of the Time Relaxation Model with high order deconvolution operator. Results in Applied Mathematics (2020) 100111, https://doi.org/10.1016/j.rinam.2020.100111.

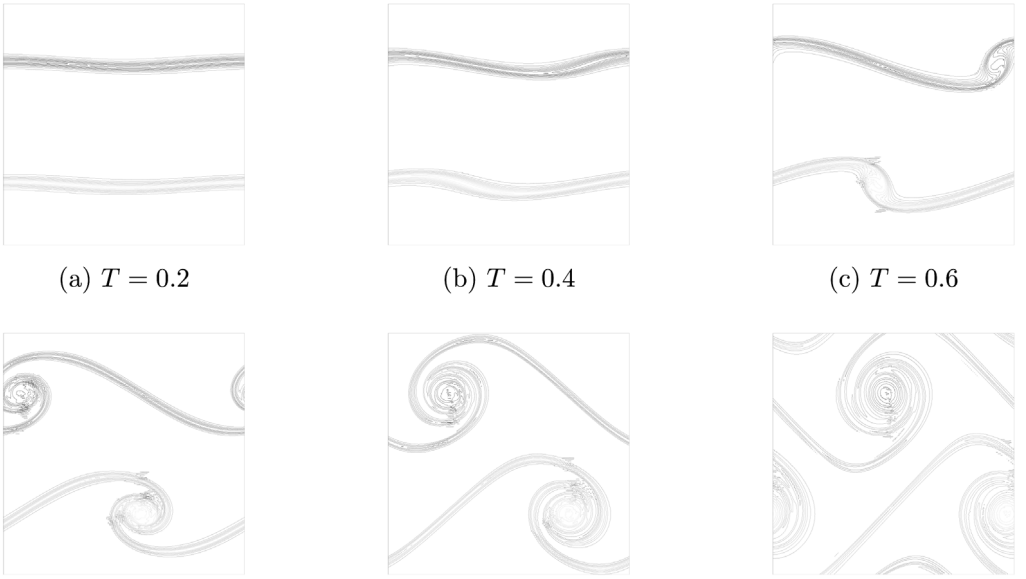

(a) $T = 0.2$ (b) $T = 0.4$ (c) $T = 0.6$

(d) $T = 0.8$ (e) $T = 1.0$ (f) $T = 1.2$

Fig. 10. Vorticity for the NSE on a fine mesh (m = 250).

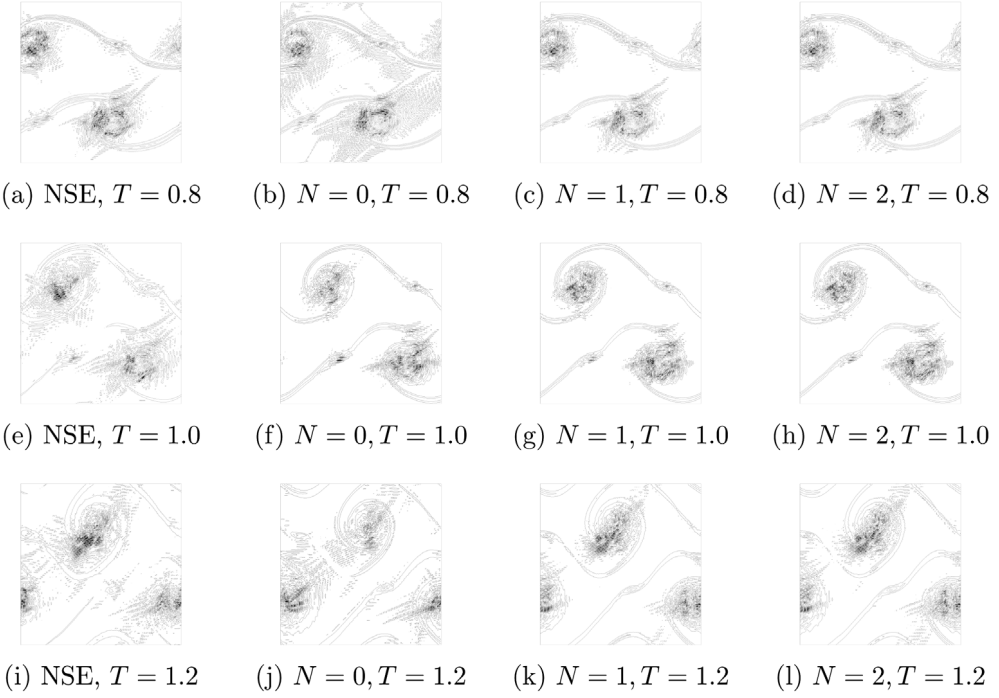

(a) NSE, $T = 0.8$ (b) $N = 0, T = 0.8$ (c) $N = 1, T = 0.8$ (d) $N = 2, T = 0.8$

(e) NSE, $T = 1.0$ (f) $N = 0, T = 1.0$ (g) $N = 1, T = 1.0$ (h) $N = 2, T = 1.0$

(i) NSE, $T = 1.2$ (j) $N = 0, T = 1.2$ (k) $N = 1, T = 1.2$ (l) $N = 2, T = 1.2$

Fig. 11. Vorticity for NSE Vs. TRM for various N, $\chi = 0.1$, scaled $\delta_N = \delta_0\sqrt{N+1}$.

4.2.2. Parameter sensitivity computations

In this section, we provide a computational assessment of the parameter sensitivity of TRM model with respect to the variation of χ values for the van Cittert deconvolution operator of orders $N = 0$, 1, and 2. A detailed analysis of TRM sensitivity with respect to the time relaxation parameter χ using the Continuous Sensitivity Equation Method, CSEM, for $N = 0$ can be found in [22]. In this paper, we derive the sensitivity equations by differentiating the TRM equations

Please cite this article as: J. Belding, M. Neda and F. Pahlevani, Computational study of the Time Relaxation Model with high order deconvolution operator. Results in Applied Mathematics (2020) 100111, https://doi.org/10.1016/j.rinam.2020.100111.

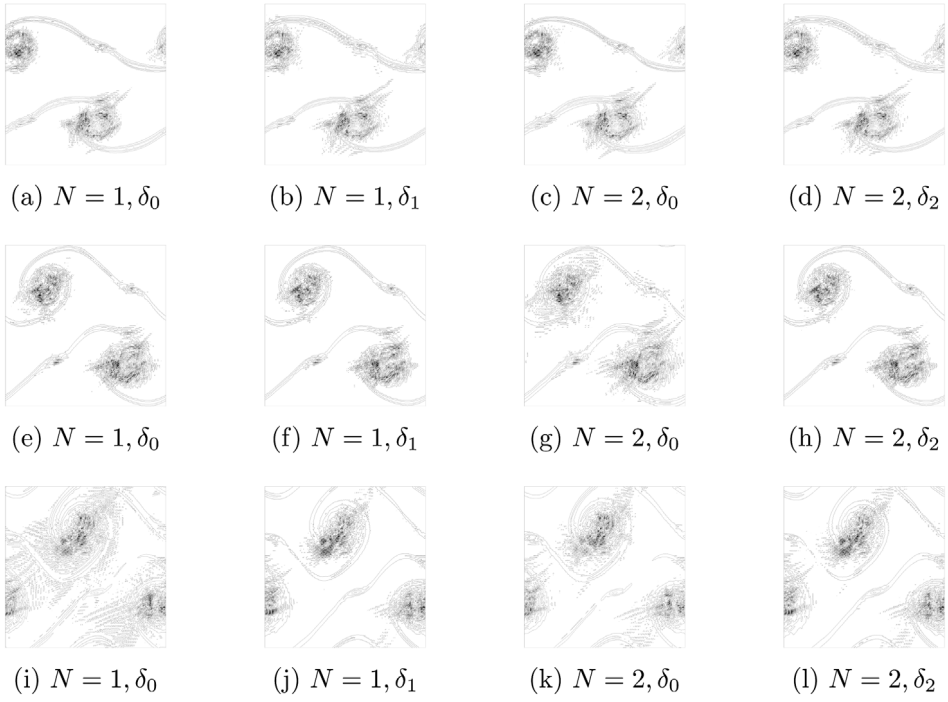

Fig. 12. Vorticity for $N = 1, 2$, $\chi = 0.1$, unscaled δ_0 and scaled δ_N, at times $T = 0.8$ (first row), $T = 1.0$ (second row), and $T = 1.2$ (third row).

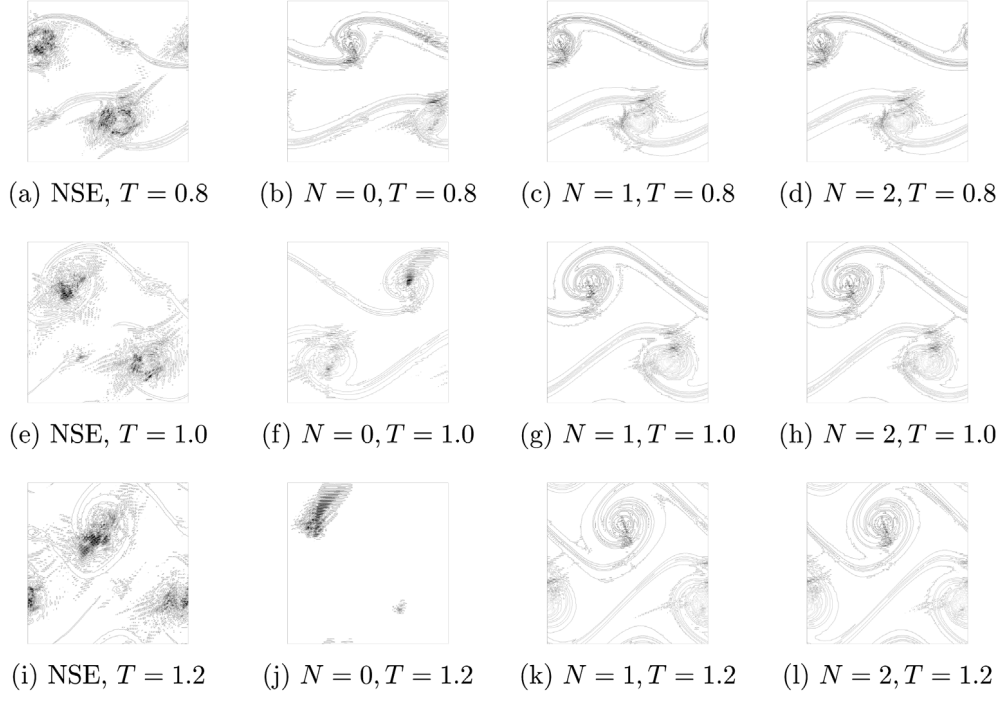

Fig. 13. Vorticity for NSE Vs. TRM for various N, $\chi = 1$, scaled $\delta_N = \delta_0\sqrt{N+1}$.

Please cite this article as: J. Belding, M. Neda and F. Pahlevani, Computational study of the Time Relaxation Model with high order deconvolution operator. Results in Applied Mathematics (2020) 100111, https://doi.org/10.1016/j.rinam.2020.100111.

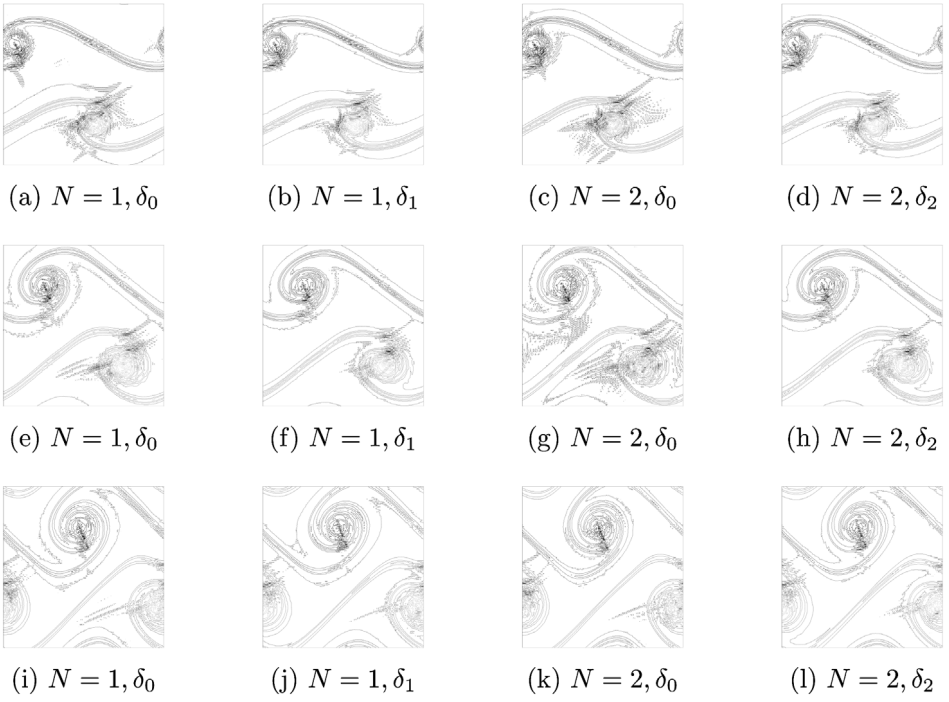

(a) $N = 1, \delta_0$ (b) $N = 1, \delta_1$ (c) $N = 2, \delta_0$ (d) $N = 2, \delta_2$

(e) $N = 1, \delta_0$ (f) $N = 1, \delta_1$ (g) $N = 2, \delta_0$ (h) $N = 2, \delta_2$

(i) $N = 1, \delta_0$ (j) $N = 1, \delta_1$ (k) $N = 2, \delta_0$ (l) $N = 2, \delta_2$

Fig. 14. Vorticity for $N = 1$, 2, $\chi = 1$, unscaled δ_0 and scaled δ_N, at times $T = 0.8$ (first row), $T = 1.0$ (second row), and $T = 1.2$ (third row).

(1.1)–(1.2) with respect to χ. Thus given $(\mathbf{u}, p)$, we find $(\mathbf{s}, r)$ such that

$$\begin{aligned}
&\mathbf{s}_t + \mathbf{u}\cdot\nabla\mathbf{s} + \mathbf{s}\cdot\nabla\mathbf{u} + \nabla r - \nu\triangle\mathbf{s} + (\mathbf{u} - G_N\bar{\mathbf{u}}) + \chi(\mathbf{s} - G_N\mathbf{w}) = 0, \ \text{in } \Omega\times[0,T],\\
&\nabla\cdot\mathbf{s} = 0, \ \text{in } \Omega\times[0,T],\\
&\mathbf{s} = 0, \ \text{on } \partial\Omega\times[0,T].
\end{aligned} \tag{4.1}$$

where $\mathbf{s} = \dfrac{\partial\mathbf{u}}{\partial\chi}$, $r = \dfrac{\partial p}{\partial\chi}$ and $\mathbf{w} = \dfrac{\partial\bar{\mathbf{u}}}{\partial\chi}$. Here, $\mathbf{w}$ satisfies the following sensitivity filtering equation,

$$\begin{aligned}
-\delta^2\triangle\mathbf{w} + \mathbf{w} &= \mathbf{s}, \text{ in } \Omega,\\
\mathbf{w} &= 0, \text{ on } \partial\Omega.
\end{aligned} \tag{4.2}$$

In order to obtain the solution for (4.1) we need to couple (1.1) with (4.1) as, $\mathbf{u}$ appears in the sensitivity equation. The fully discretized variational formulation for the sensitivity using Crank–Nicolson is to find $\mathbf{s}_h^{n+1} \in V^h$ satisfying:

$$\begin{aligned}
&\frac{1}{\triangle t}(\mathbf{s}_h^{n+1} - \mathbf{s}_h^n, \mathbf{v}_h) + \nu a(\mathbf{s}_h^{n+1/2}, \mathbf{v}_h) + b^*(\mathbf{s}_h^{n+1/2}, \mathbf{u}_h^{n+1/2}, \mathbf{v}_h) + b^*(\mathbf{u}_h^{n+1/2}, \mathbf{s}_h^{n+1/2}, \mathbf{v}_h)\\
&\quad + (\mathbf{u}_h^{n+1/2} - \bar{\mathbf{u}}_h^{n+1/2}, \mathbf{v}_h) + \chi(\mathbf{s}_h^{n+1/2} - \mathbf{w}_h^{n+1/2}, \mathbf{v}_h) = 0, \quad \forall\mathbf{v}_h \in V^h
\end{aligned} \tag{4.3}$$

$$\delta^2(\nabla\mathbf{w}_h^{n+1}, \nabla v_h) + (\mathbf{w}_h^{n+1}, \mathbf{v}_h) = (\mathbf{s}_h^{n+1}, \mathbf{v}_h), \quad \forall\mathbf{v}_h \in V^h \tag{4.4}$$

The existence, stability, and convergence analysis of the finite element solution of the above scheme is investigated in [22]. In the following numerical computations, we consider using sensitivity as an accuracy assessment for the approximated velocity solution with different values of parameter χ via computing $\chi\|\mathbf{s}\|_{l^2(0,1.2;L^2(\Omega))}$. This is a simple result based on the following difference quotient for the sensitivity,

$$\mathbf{s} = \frac{\partial\mathbf{u}}{\partial\chi} \approx \frac{\mathbf{u}(\chi) - \mathbf{u}(0)}{\chi}$$

where $\mathbf{u}$ is considered an implicit function of χ. Thus, $\mathbf{u}(0)$ indicates the true solution of Navier–Stokes equations while $\mathbf{u}(\chi)$ for $\chi > 0$ denotes the corresponding TRM approximation of the velocity. According to the above finite difference formula, $\mathbf{u}(\chi)$ for a given χ value is an accurate approximation to $\mathbf{u}(0)$ when $\|\mathbf{u}(\chi) - \mathbf{u}(0)\|$ is small. Thus the accuracy of $\mathbf{u}(\chi)$ can be estimated by measuring $\chi\|\mathbf{s}\|$.

The following Tables 1 and 2 contain the sensitivity values of $\chi\|\mathbf{s}\|_{l^2(0,1.2;L^2(\Omega))}$ for Reynolds number $Re = 10{,}000$ and the time relaxation parameter $\chi = 0.01$, 0.1, 1, and 10 with two choices for a fixed filter length of $\delta_0 = 5/m = 0.05$ and

Please cite this article as: J. Belding, M. Neda and F. Pahlevani, Computational study of the Time Relaxation Model with high order deconvolution operator. Results in Applied Mathematics (2020) 100111, https://doi.org/10.1016/j.rinam.2020.100111.

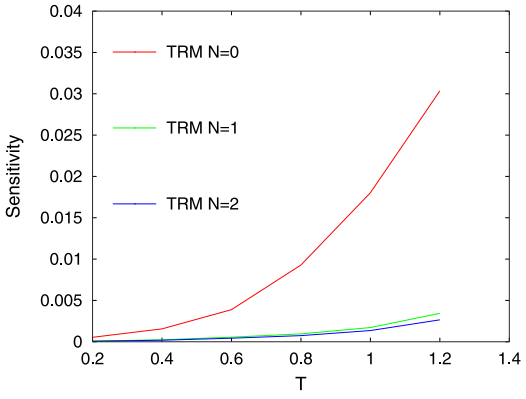

(a) $\chi = 0.01$

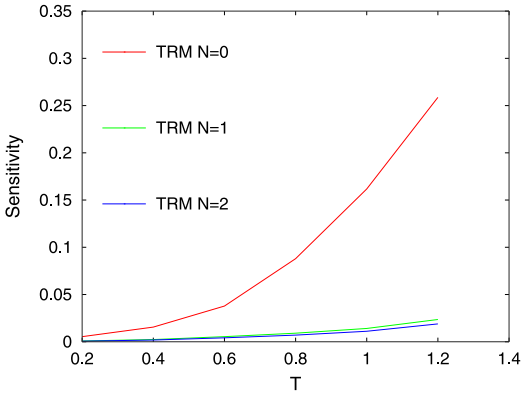

(b) $\chi = 0.1$

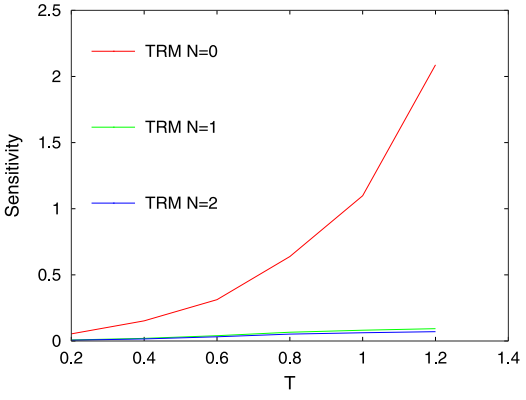

(c) $\chi = 1$

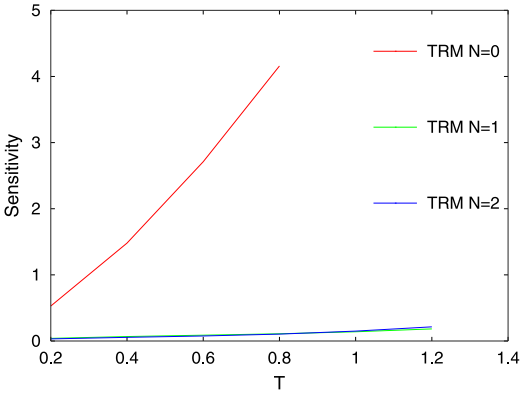

(d) $\chi = 10$

Fig. 15. Sensitivity $\chi \|\mathbf{s}\|_{l^2(0,T;L^2(\Omega))}$ values in time for unscaled $\delta_0 = \frac{5}{m}$.

Table 1
$\chi ||\mathbf{s}||_{l^2(0,1.2;L^2(\Omega))}$ values for unscaled δ_0.

χ	$N = 0$	$N = 1$	$N = 2$
0.01	3.035e−2	3.44e−3	2.655e−3
0.1	2.5865e−1	2.356e−2	1.8893e−2
1	2.08791	9.313e−2	7.0404e−2
10	–	1.8300e−1	2.13989e−1

Table 2
$\chi ||\mathbf{s}||_{l^2(0,1.2;L^2(\Omega))}$ values for scaled δ_N.

χ	$N = 0$	$N = 1$	$N = 2$
0.01	3.035e−2	4.64592e−3	4.46365e−3
0.1	2.5865e−1	3.17663e−2	3.04986e−2
1	2.08791	1.29948e−1	1.22917e−1
10	–	1.79795e−1	1.40921e−1

$\delta_N = \delta_0\sqrt{N+1}$ (i.e. $\delta_1 = \delta_0\sqrt{2}$ and $\delta_2 = \delta_0\sqrt{3}$) as well as different values of the van Cittert operator, i.e. $N = 0$, 1, and 2. The selected spatial mesh size consists of $m = 100$ subintervals in both x and y directions. All the computations are carried out with a uniform time-step $\Delta t = 0.004$ using the Taylor–Hood finite elements on the time interval $[0, 1.2]$. We note that the fixed point iteration implemented for the nonlinear term failed to converge (after 50 performed iterations) for $N = 0$ and $\chi = 10$.

Across all the N values, the least values of $\chi \|\mathbf{s}\|_{l^2(0,1.2;L^2(\Omega))}$ are associated with $\chi \leq 0.1$. Thus, we identify the interval of $[0, 0.1]$ as the interval of reliability for this parameter value. All the tested χ values in both tables show an

Please cite this article as: J. Belding, M. Neda and F. Pahlevani, Computational study of the Time Relaxation Model with high order deconvolution operator. Results in Applied Mathematics (2020) 100111, https://doi.org/10.1016/j.rinam.2020.100111.

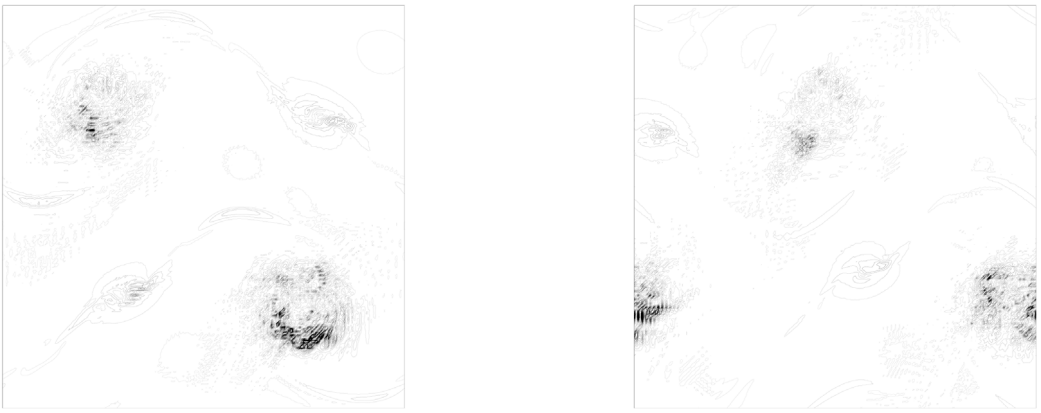

(a) $t = 1.0$ (b) $t = 1.2$

Fig. 16. Sensitivity norm of TRM for $\chi = 0.1$, $\delta = \frac{5}{m}$, $N = 1$ at $t = 1.0, 1.2$.

improved sensitivity value for higher order van Cittert operator, i.e. for larger N values, indicating a better accuracy for the approximated velocity $\mathbf{u}$.

With this same experiment, the progression of sensitivity values across different times, $t = 0.2, 0.4, 0.6, 0.8, 1.0$, and 1.2, for $\delta_0 = 5/m = 0.05$ was tested. The plots in Fig. 15 present the results of these computations for $\chi = 0.01, 0.1, 1, 10$ and $N = 0, 1$, and 2. For any χ values, the sensitivity values at all times are smaller for larger values of N. For all N and χ values, $\chi \|\mathbf{s}\|_{l^2(0,T;L^2(\Omega))}$ increases in value as T progresses to 1.2.

Fig. 16 shows the norm of sensitivity of TRM with $\chi = 0.1$ at times $t = 1.0$ and $t = 1.2$ for Re=10,000, with unscaled $\delta_0 = 5/m$, and for order of deconvolution $N = 1$. We can see that the sensitivity, i.e. velocity deviations with respect to χ, are concentrated in areas of vorticity actions.

5. Conclusions

In this paper we computationally studied the so called time relaxation model, TRM, and its sensitivity. The model is regularizing the flow at higher Reynolds number through filtering and deconvolution effects that are added as an additional term to the Navier–Stokes equations. The TRM and its corresponding sensitivity equations were both discretized using finite element in space and second order Crank–Nicolson method in time. We tested the performance of this model with different deconvolution orders, i.e. $N = 0$, 1, and 2, using the step problem and the shear layer roll-up benchmark problem. Our computations using the Olson's suggested average filter length scale produced improved results and confirmed the positive effect of such scaling for higher deconvolution order N especially for the shear layer problem where the noise was reduced. In the step problem not many different scale sizes of rotational structure are present, the flow away from the step is smooth with no eddies at all, so the effect of the average length scale for higher order deconvolution was not that visible. The sensitivity computations of TRM with respect to the variation of parameter χ verified the range of this parameter's values for a reliable approximated solution. We noted that the sensitivity was lower as the order of deconvolution was increased.

Declaration of competing interest

The authors declare that they have no known competing financial interests or personal relationships that could have appeared to influence the work reported in this paper.

Acknowledgment

We are thankful to Dr. Eric Olson for sharing his insights and results on the effective average scaling for the filter width.

References

[1] Layton W, Neda M. Truncation of scales by time relaxation. J Math Anal Appl 2007;325(2):788–807.
[2] Stolz S, Adams N, Kleiser L. The approximate deconvolution model for les of compressible flows and its application to shock-turbulent-boundary-layer interaction. Phys Fluids 2001;13:2985.
[3] Stolz S, Adams N, Kleiser L. An approximate deconvolution model for large eddy simulation with application to wall-bounded flows. Phys Fluids 2001;13:997.

Please cite this article as: J. Belding, M. Neda and F. Pahlevani, Computational study of the Time Relaxation Model with high order deconvolution operator. Results in Applied Mathematics (2020) 100111, https://doi.org/10.1016/j.rinam.2020.100111.

[4] De S, Hannasch D, Neda M, Nikonova E. Numerical analysis and computations of a higher accuracy time relaxation fluid flow model. Int J Comput Math 2008;1–22.
[5] Dunca A, Neda M. Numerical analysis of a nonlinear model of fluids. J Math Anal Appl 2014;420:1095–115.
[6] Neda M. Discontinuous time relaxation method for the time dependent Navier–Stokes equations. Adv Numer Anal 2010;419021:1–21.
[7] Neda M, Pahlevani F, Waters J. Sensitivity analysis and computations of the time relaxation model. J Adv Appl Math Mech 2015;7:89–115.
[8] Davis L, Neda M, Pahlevani F, Waters J. Fluid models and parameter sensitivities: Computations and applications. Int J Novel Ideas: Math 2017;1:12–39.
[9] Bertero M, Boccacci P, Koenig A. Introduction to inverse problems in imaging. Opt Photonics News 2001;12:46–7, 10.
[10] Ervin V, Layton W, Neda M. Numerical analysis of a higher order time relaxation model of fluids. Int J Numer Anal Model 2007;4(3):648–70.
[11] Olson E. Model error in the LANS-alpha and NS-alpha deconvolution models of turbulence. Int J Numer Anal Model 2018;15(4):811–33.
[12] Kaya-Merdan S, Manica C. Convergence analysis of the finite element method for a fundamental model in turbulence. M3AS 2012;22:11, 24 pp.
[13] Bowers A, Rebholz L. Increasing accuracy and efficiency in FE computations of the Leray-deconvolution model. Numer Methods Partial Differential Equations 2012;28(2):720–36.
[14] Connors J. Convergence analysis and computational testing of the finite element discretization of the Navier–Stokes-alpha model. Numer Methods Partial Differential Equationss 2009.
[15] Manica C, Neda M, Olshanskii M, Rebholz L. Enabling numerical accuracy of Navier–Stokes-α through deconvolution and enhanced stability. ESAIM Math Model Numer Anal 2010;45(2):277—-307.
[16] Dunca A, Epshteyn Y. On the stolz–adams deconvolution model for the large-eddy simulation of turbulent flows. SIAM J Math Anal 2006;37(6):1890–902.
[17] Layton W, Manica C, Neda M, Rebholz L. Numerical analysis of a high accuracy Leray-deconvolution model of turbulence. Numer Methods Partial Differential Equations 2008;24:555–82.
[18] Gunzburger M. Finite Element Methods for Viscous Incompressible Flows - a Guide To Theory, Practices, and Algorithms. Academic Press; 1989.
[19] Fischer P, Mullen J. Filter-based stabilization of spectral element methods. C R Acad Sci Paris Sér I Math 2001;332:265–70.
[20] Bell J, Collela P, Glaz H. A second-order projection method for the incompressible Navier-Stokes equations. Internat J Numer Methods Fluids 1989;8:537–57.
[21] Brown D, Minion M. Performance of under-resolved two-dimensional incompressible flow simulations. J Comput Phys 1995;122:283–8.
[22] Neda M, Pahlevani F, Waters J. Sensitivity analysis of the time relaxation model. Appl Math Mech 2015;7:89–115.

Please cite this article as: J. Belding, M. Neda and F. Pahlevani, Computational study of the Time Relaxation Model with high order deconvolution operator. Results in Applied Mathematics (2020) 100111, https://doi.org/10.1016/j.rinam.2020.100111.